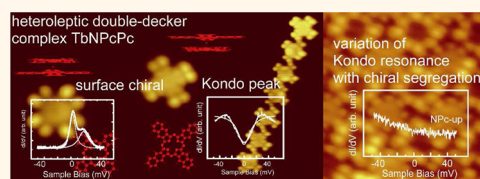


Variation of Kondo Peak Observed in the Assembly of Heteroleptic 2,3-Naphthalocyaninato Phthalocyaninato Tb(III) Double-Decker Complex on Au(111)

Tadahiro Komeda,^{†,§,*} Hironari Isshiki,^{†,‡} Jie Liu,^{†,‡} Keiichi Katoh,^{‡,§} Minoru Shirakata,[‡] Brian K. Breedlove,[‡] and Masahiro Yamashita^{†,§}

[†]Institute of Multidisciplinary Research for Advanced Materials (IMRAM, Taten) and [‡]Department of Chemistry, Graduate School of Science, Tohoku University, 2-1-1, Katahira, Aoba-Ku, Sendai 980-0877, Japan and [§]JST, CREST, 4-1-8 Honcho, Kawaguchi, Saitama 332-0012, Japan

ABSTRACT By using scanning tunneling microscopy (STM), we studied the heteroleptic double-decker complex TbNPcPc (NPC = naphthalocyaninato and Pc = phthalocyaninato), where two different planar ligands sandwich a Tb(III) ion and an unpaired π electron causes Kondo resonance upon adsorption on the Au(111) surface. Kondo resonance is a good conductance control mechanism originating from interactions between conduction electrons and a localized spin. Two types of adsorption geometries appear depending on which side contacts the substrate surface, which we call Pc-up and NPC-up molecules. They make intriguing molecular assemblies by segregation. In addition, different adsorption geometries and molecular assemblies provide a variety of spin and electronic configurations. Pc-up and NPC-up molecules both showed the Kondo resonance when they were isolated from other molecules, but their Kondo temperatures were different. A one-dimensional chain composed of only NPC-up molecules was found, in which the dI/dV plot showed a conversion from the Kondo peak to a dip at the Fermi energy. In addition, a two-dimensional lattice with an ordering of Pc-up and NPC-up molecules in an alternative manner was observed, in which no Kondo peak was detected in the molecule. The absence of the Kondo peak was accounted for by the change of azimuthal rotational angle of the two ligands of both molecules. The results imply that a molecule design and adsorption configuration tailoring can be used for the spin-mediated control of the electronic conductance of the molecule.



KEYWORDS: scanning tunneling microscopy · scanning tunneling spectroscopy · Kondo resonance · chirality · phthalocyanine · single-molecule magnet

Molecular spintronics devices utilize the freedom of charge as well as the spin of electrons.¹ Using molecules in such devices makes it possible to control precisely the spin distribution via molecule synthesis and/or control of the molecule ordering in films. For instance, much research has gone into the synthesis of molecules linked by noncovalent bonding.^{2,3} For a control of molecule ordering, the use of characteristic features of surfaces has been developed. When a molecule is adsorbed on a surface, it loses the freedom of flipping. Thus, identical planar molecules can adsorb on a surface face up and down, which have different chemical natures.

In this report, we synthesized the heteroleptic double-decker complex TbNPcPc (NPC = naphthalocyaninato and Pc = phthalocyaninato), in which two different planar ligands sandwich a Tb(III) ion with a 1/2 spin π radical in the ligands, and studied its structure and spin properties by using low-temperature scanning tunneling microscopy (STM). Upon adsorption on a surface, two types of adsorption geometries appear depending on which side contacts the substrate surface. The molecule whose NPC ligand is in the vacuum side is called the NPC-up molecule. The mixture of NPC-up and Pc-up molecules makes intriguing molecular assemblies by segregation, including straight chain consisting of only NPC-up

* Address correspondence to komeda@tagen.tohoku.ac.jp.

Received for review September 1, 2012 and accepted January 30, 2013.

Published online January 30, 2013
10.1021/nn304035h

© 2013 American Chemical Society

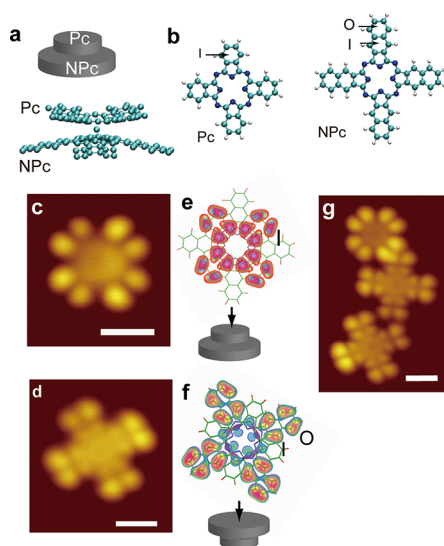


Figure 1. (a,b) Models of the TbNPcPc double-decker molecules. “I” and “O” in b specify the position of the outer phenyl rings. (c–f) STM images and DFT simulated images of isolated Pc-up and NPc-up molecules. (g) STM image of aggregates. White bars in (c), (d), and (g) are 1 nm.

molecules and a film in which NPc-up and Pc-up molecules alternate. In dI/dV spectra, a Kondo resonance, which is a good conductance control mechanism originating from interactions between conduction electrons and a localized spin,⁴ was detected when the STM tip was over ligands of isolated NPc-up and Pc-up molecules. The Kondo peak was converted into a dip at the Fermi level in the 1D chain and disappeared in the 2D film. The results imply that a molecule design and adsorption configuration tailoring can be used for the spin-mediated control of the electronic conductance of the molecule.

RESULTS AND DISCUSSION

The structure of a 2,3-naphthalocyaninato phthalocyaninato Tb(III) double-decker complex (TbNPcPc) molecule is shown in Figure 1a, in which Pc and NPc ligands sandwich a Tb(III) ion. In the model, the smaller Pc and larger NPc ligands stack parallel to each other. As can be seen in the side view, Pc and NPc ligands adopt a bent configuration with respect to each other. Top views of both ligands are shown in Figure 1b. The difference between the Pc and NPc ligands is the four phenyl rings marked with an “O” in the figure extending from “I”. Upon adsorption on a Au(111) surface, the freedom of the flipping is lost. Thus, adsorbed molecules can have two distinct adsorption configurations.

Pc-up and NPc-up molecules can be distinguished in STM images, as shown in Figure 1c,d. On the basis of the length of the diagonal (~ 1.5 and ~ 2.0 nm for Pc and NPc, respectively), we assigned the images in Figure 1c,d to Pc-up and NPc-up molecules, respectively. This was further confirmed *via* comparisons with simulated STM images created by using density

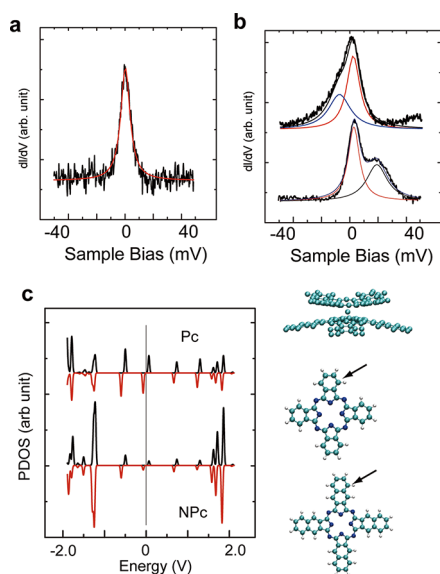


Figure 2. (a,b) dI/dV spectra over an isolated molecules of (a) Pc-up and (b) NPc-up. Solid lines were fitted using a Lorentzian function. (c) Spin-resolved PDOS vs energy plots of the carbon atoms of Pc and NPc ligands of TbNPcPc, indicated by arrows. Red and black lines are for major and minor spin components.

functional theory (DFT). Simulated STM images of Pc-up and NPc-up molecules are shown in Figure 1e,f, respectively, with the marks of “I” and “O”.

Although an ordered film could not be obtained *via* deposition at room temperature, small clusters were. Figure 1g shows aggregates of Pc-up and NPc-up molecules. The separation between Pc-up and NPc-up molecules was determined to be ~ 1.7 nm. The lobes of the Pc-up molecules dominate those of the NPc-up molecules when they are close to each other due to the difference in the DOSs of the lobes.

In the dI/dV spectra of TbNPcPc molecules, a Kondo resonance was observed near the Fermi level. Kondo peaks have been observed in spectra of single atoms,^{5–10} single molecules,^{11–15} and quantum dots.¹⁶ We have reported a Kondo feature as a zero-bias peak (ZBP) near the Fermi level in the dI/dV spectra of the single-molecule magnet (SMM) TbPc₂, which originates from the unpaired spin in the π orbitals of the Pc ligands.¹⁷ Similar ZBPs were observed in the spectra of both Pc-up (Figure 2a) and NPc-up molecules (Figure 2b) when the STM tip was placed over the lobes of the ligands. The origin of the Kondo peaks was attributed to an unpaired π orbital for both molecules, which was supported by the electronic structure calculated using a spin-resolved DFT method. The results of the spin-resolved DFT calculations are shown in Figure 2c, in which the partial density of states (PDOS) was calculated at the positions indicated by the arrows. At the Fermi level, a singly occupied state for both molecules was observed, which supports the existence of spins on both ligands. In addition, the plots of the PDOSs for the two molecules are similar,

indicating that, when phenyl O is added to I, the energies of the eigenstates barely change and that the distributions of the corresponding molecular orbitals are extended. The latter is consistent with the distribution of the bright areas in Figure 1e,g.

However, the widths of the Kondo peaks of Pc-up and NPC-up molecules observed at the lobes were different. Figure 2a,b shows fitted Kondo peaks with Lorentzian functions. The widths of the main peaks were determined to be ~ 8 and ~ 12 mV for Pc-up and NPC-up molecules, respectively. The widths can be converted to T_K by using a formula for the temperature dependence of the Kondo peak width ($\Gamma(T)$), which is based on Fermi liquid theory:¹⁸ $\Gamma(T) = 2((\pi k_B T)^2 + 2(k_B T_K)^2)^{1/2}$, where k_B is the Boltzmann constant. The values of T_K were calculated to be ~ 32 and ~ 48 K for Pc-up and NPC-up molecules, respectively. The difference in T_K is explained below.

We analyze the difference of T_K observed at NPC-up and Pc-up molecules by considering the distance between the vacuum side ligand and the Au substrate. For the TbPc₂ molecule, we previously reported that the unpaired π orbital, that is, the origin of the Kondo resonance, is distributed in the vacuum side ligand.¹⁷ This is also the case for the current molecule. As already mentioned, this molecule has a bent configuration. The estimation of the absolute height of the vacuum side ligand from the substrate is not possible since DFT calculation cannot calculate the dispersion force of the van der Waals interaction. However, it is possible to argue the height difference of the NPC-up and Pc-up from the results of the DFT calculation for an isolated molecule in the vacuum. The NPC ligand has a larger size than the Pc ligand, and both have a similar bent angle. Thus, we estimated that the vacuum side ligand of the Pc-up molecule is higher than that of the NPC-up molecule by ~ 1 Å.

In the Kondo physics, it is known that T_K can be expressed by the following formula, $T_K \propto \exp(-\pi|\varepsilon|/m\Gamma)$, where Γ is the peak width of the spin impurity originated from a hybridization with the surface, ε is the energy relative to E_F , and m is the degeneracy of the orbital.^{19,20} Γ decreases with an increase of the distance between the vacuum ligand and the substrate due to the decrease of the hybridization between the two. Thus, with the increase of the distance, lower T_K is expected. This can account for the lower T_K for the Pc-up molecule than that for the NPC-up molecule since the ligand of the former case is ~ 1 Å higher than that of the latter case.

For a NPC-up molecule, there often appeared additional peaks on both sides of the Kondo peak. They are depicted by black solid lines as a fitting line in Figure 2b. Two spectra were obtained at the lobe positions of different NPC-up molecules. The energies of peaks were read at -7 and 19 mV for upper and lower spectra, respectively. They were seldom observed for Pc-up molecules. Side bands of the Kondo

peak were reported by Torrente *et al.* for a TTF-TCNQ molecule whose origin was attributed to a vibration-assisted Kondo resonance and off-resonant inelastic tunneling process of a vibration excitation.¹⁵ We speculate that a similar vibrational excitation is a mechanism for the appearance of the side bands in our experiment. A previous report showed the energy of the metal–N stretching mode at 18.5 mV,²¹ and the lower peak at 7 meV can be assigned to a substrate–molecule vibrational mode.

However, their intensity is not symmetric around the Kondo peak. This should be related to the yield of vibration excitation process which depends on the coupling between initial and final electronic states of tunneling and the vibrational mode.^{15,22,23} Thus the peak intensity that is related to the vibration excitation should be affected by the distribution of the PDOS of these electronic states which do not have to be symmetric around the Fermi level.

In addition, the inelastic excitation is not limited to the excitation of vibrational modes. For example, spin excitation of the center Tb atom can be coupled to the Kondo resonance that should appear in a few tens of millielectronvolts.²⁴ It requires further study to make a clear assignment of these side peaks.

In the aggregates of Pc-up and NPC-up molecules like that of Figure 1g, although the distance between the molecules is shorter, the Kondo peaks were scarcely different from those of the isolated molecules.

When TbNPcPc molecules were deposited on a slightly annealed substrate at ~ 80 °C, ordered chain structures formed, as shown in Figure 3a. Intriguingly, the chain is composed of only NPC-up molecules, as illustrated in Figure 3b. A detailed model of the adsorption configuration is shown in Figure 3c. The chain was parallel to the direction which can be expressed as $-4\mathbf{s} + 9\mathbf{t}$ using the unit vectors of substrate \mathbf{s} and \mathbf{t} (see Figure 3c), which are slightly tilted from the $[1\bar{1}\bar{2}]$ direction. The chains were preferentially formed at the face-centered cubic sites sandwiched by the soliton wall of the Au(111) reconstructed surface,²⁵ and the centers of the molecules were separated by ~ 2.2 nm. The symmetry line was tilted by $\sim 75^\circ$ from the $[1\bar{1}\bar{2}]$ direction (see Figure 3a), which can be explained by a model that the lower NPC symmetry line is parallel to the $[1\bar{1}0]$ direction and upper and lower ligands are rotated 45° from each other.

The dI/dV spectra of the chain molecules are shown in Figure 3e, whose measurement positions are indicated by the arrows in Figure 3d. The spectrum obtained over an edge molecule (plot I in Figure 3e) showed a protrusion similar to that obtained over an isolated molecule, but the peak width was broadened and a higher T_K (~ 60 K) was estimated.

Variations of width and shape of a Kondo peak with an approach of additional spins have been examined in many systems. Wahl *et al.* showed a variation of Kondo

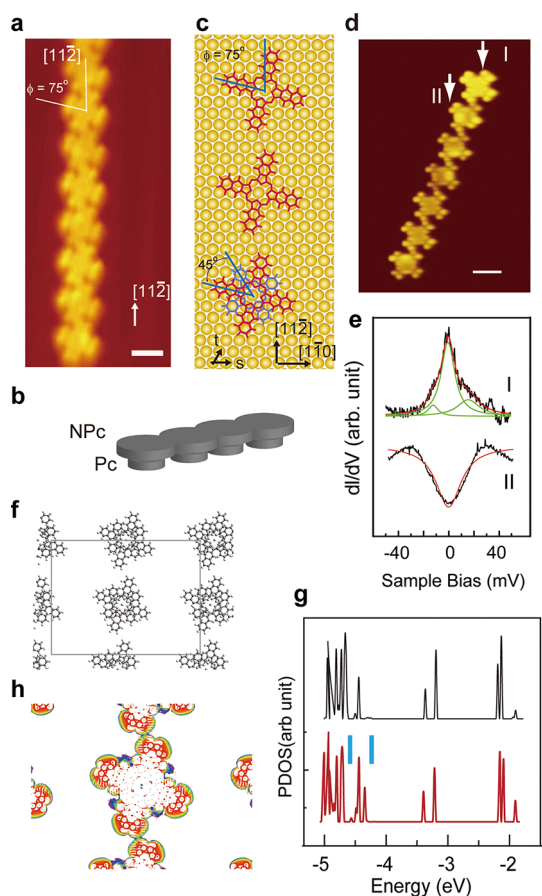


Figure 3. (a) STM image of NPC-up chain. White bar = 1 nm. (b,c) Schematic models of the structure of the chain in (a). (d) High-resolution STM image of the NPC-up chain. White bar = 1 nm. (e) dI/dV spectra measured at I and II in (d). (f) Model of 1D chain of NPC-up molecules used for DFT calculation (free-standing). (g) PDOS vs energy plots for isolated NPC-up molecule (top, black) and for NPC-up 1D chain level. (f) Spin-resolved PDOSs vs energy plots calculated over Pc-up and NPC-up molecules. (g) Change in the peak positions of the SOMO and HOMO levels versus azimuthal angle between upper and lower ligands, which are determined by using DFT calculations.

peaks of a Co atom on Cu(100) by controlling the coupling between the spins of individual cobalt adatoms with their surroundings.⁹ Though compact dimer Co suppresses the Kondo resonance due to strong ferromagnetic coupling between Co atoms, the spectrum on the next nearest neighbor dimer shows a distinct Kondo resonance at the Fermi level, whose peak width is broadened compared to that of the isolated Co adatom. The broadening was accounted for by an antiferromagnetic coupling between the two Co adatoms. Tsukahara *et al.* have shown the Kondo variation of a FePc molecule on Au(111) with a formation of a two-dimensional lattice. A sharp Kondo peak appears in the single-impurity regime, which broadens and splits as the lattice builds up, which was related to Rudermann–Kittel–Kasuya–Yosida (RKKY) coupling between the molecular spins.²⁶

The broadening of the Kondo resonance observed at the edge molecule of the 1D chain in our

experiment originates from the spin–spin interaction.

On the other hand, the spectra obtained over the molecules inside of the chain (plot II in Figure 3e) showed a dip around the Fermi level, whose width was ~ 30 mV at the half-maximum. We consider a mechanism of the appearance of the dip. First we examine the Fano resonance. In the STM configuration, electrons tunnel from tip to substrate either directly or by interacting with the spin impurity. They show a quantum interference to cause a dip in STS, which is known as Fano resonance and has been studied theoretically^{18,27–29} and experimentally.^{12,30,31}

The spectrum of Fano resonance was analyzed using the following equations:^{18,28,29}

$$dI(V)/dV \propto \frac{\rho_0(\varepsilon+q)^2}{\varepsilon^2+1} \quad \text{and} \quad \varepsilon = \frac{eV - \varepsilon_0}{\Gamma}$$

where q is the Fano parameter, ε_0 is the peak position, and Γ is the width of the peak. From the fitted curve in plot II of Figure 3e, Γ and q were determined to be 12 mV and 0.012, respectively. The estimated T_K of ~ 48 K, deduced from $\Gamma = k_B T_K$, is almost same as that of an isolated NPC-up.

The fitting result was not satisfactory. First, the fitted curve does not quite reproduce the observed plot, which seemingly consists of two components. Second, a small value of q , 0.012, is obtained. In the Fano dip arguments, small q is often attributed to the case where the direct tunneling from the tip to the substrate dominates the tunneling process.^{18,27–29} Since the Kondo resonance is caused by the unpaired π orbital in the upper ligand for the current system, the dominance of the direct tunneling seems unrealistic.

However, Hualde *et al.* demonstrated that the ligand–ligand interaction can explain the dip formation.^{32–34} To examine whether their analysis can be applied to our system, we first investigate the ligand–ligand interaction in the 1D chain observed in our experiment.

Recently, the Berndt group have reported a significant change of STS spectra of FePc molecules when they formed a 6×3 superstructure.³⁵ The origin was attributed to the variation of molecule–substrate interaction with the appearance of molecule–molecule interaction in the 6×3 superstructure. In order to estimate electronic configuration, they calculated electronic states of the FePc molecules both in the isolated state and in the free-standing 6×3 film. The calculation in the vacuum was preferred since DOS of the substrate obscured the direct visualization of the molecule–molecule interactions.

Following their analysis, we executed electronic state calculation for a free-standing chain of NPC molecules. The model is depicted in Figure 3f, in which the NPC molecules were separated by 2.2 nm parallel to the chain direction and 3.5 nm perpendicular to that.

The isolated molecule was modeled by expanding the distance from 2.2 nm to a larger distance.

The result of the calculation is shown in Figure 3g. We can see a noticeable change in the energy range between the blue bars of the Figure 3g, in which more states were identified for the case of the chain compared to that of the single molecule. This is rational because the single-molecule state should be split into multiple peaks when a molecule–molecule interaction appears. The calculated integrated local DOS is depicted in Figure 3h for the energy region between the blue lines. The isosurface clearly shows the overlapping of the two NPC.

We further examined this model to check whether the spin of the NPC-up molecule survives after the formation of the 1D chain of NPC-up molecules. As explained in the Supporting Information, the spin-resolved DFT calculation showed that the unpaired π orbital spin remains after the formation of the 1D chain.

A similar PDOS variation and overlapping of wave functions of molecules were reported for an isolated and 6×3 FePc molecule assembly.³⁵ In there, it was claimed that the molecule–substrate interaction was weakened with the increase of molecule–molecule interaction, which was followed by a lifting of the molecular layer. We consider that a similar situation occurs in the 1D chain of our system; ligand–ligand interaction appears which weakens molecule–substrate interaction.

We like to return to the discussion of the molecule–molecule interaction and Fano dip. Hualde *et al.* analyzed the effect of ligands for the Kondo resonance observed for CoPc/Au(111)¹¹ and TBrPP-Co/Cu(111).¹² Both molecules consist of a center Co atom and a ligand with four lobes, but the Kondo resonances show a large difference. For the former case, the Kondo peak is absent for a nonperturbed molecule, but it appears after the modification of the ligand by injecting tunneling electrons into the molecule. For the latter molecule, a Fano dip was observed. They considered that quantum interference between two tunneling paths, which are tip/Co/metal substrate and tip/Co/lobe/metal substrate, is crucial for the appearance and disappearance of the Kondo resonance and switching between Kondo peak and dip. Since the relative contribution of tip/Co/lobe/metal substrate path is stronger in the case of TBrPP-Co than that of CoPc, the Fano dip appears. They concluded that the role of the molecular lobes is not only to participate in the screening of the spin at the Co atom, as the metallic surface does, but also contributing to change dips into peaks or even to drive the system in/out of the Kondo regime.^{32–34}

If we compare our system to these cases, an unpaired π orbital and neighbor molecules correspond to the Co atom and the lobes, respectively. The appearance of molecule–molecule overlapping in the 1D chain corresponds to the enhanced Co–lobe interaction in

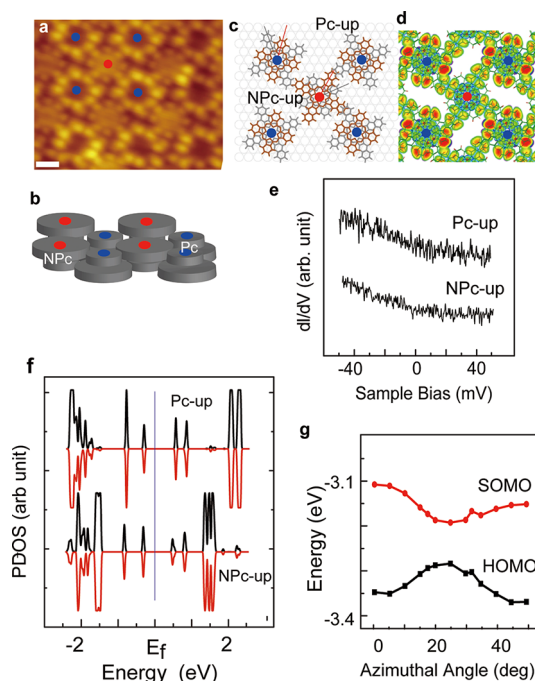


Figure 4. (a) STM image of a TbNPCPc film. Blue and red dots correspond to Pc-up and NPC-up molecules, respectively. White bar = 1 nm. (b) Schematic model of the film in (a). (c) Model of the ordered structure on a Au(111) surface. Top and bottom ligands are colored brown and gray, respectively. (d) Simulated STM image from DFT calculations. Blue and red dots correspond to those in (a). (e) dI/dV spectra near the Fermi molecule (lower, red). (f) Plot of isosurface of integrated PDOS in the energy range between two blue lines of (g).

the TBrPP-Co molecule. Consequently, we can expect the appearance of a Fano dip in the 1D chain if we follow the above discussion which claims that the surrounding ligand can change the peak and dip of the Kondo peak. The appearance of spin–spin interaction at the edge molecule and ligand–ligand overlapping effect for the inside-of-chain molecule is switched by the relative strength of those interactions. Larger contribution of the latter interaction for the inside-of-chain molecule is due to a higher coordination number, while the spin–spin interaction cannot increase in a straightforward manner with the coordination number as discussed by Wahl *et al.*⁹ In addition, we speculate that the effect of spin–spin interaction also exists in the Fano dip, which can split the peaks as Tsukahara *et al.* observed.²⁶ This effect might make the fitting of the dip by a single Fano dip difficult.

Deposition at a substrate temperature of $\sim 80^\circ\text{C}$ led to the formation of a well-ordered two-dimensional (2D) film, an STM image of which is shown in Figure 4a. We identified two different molecules in the image, which are marked with red and blue circles. The lattice vectors u and v of the film were determined in relations to the unit vectors of the Au(111) surface, s and t (see Figure 3c):

$$\begin{pmatrix} u \\ v \end{pmatrix} = \begin{pmatrix} 9 & 0 \\ -4 & 9 \end{pmatrix} \begin{pmatrix} s \\ t \end{pmatrix}$$

assuming that molecules are at 0 and at the center of the unit rhombohedra $2.5s + 4.5t$ in the unit cell.

The image of the blue molecule is identical to that of an isolated Pc-up molecule (see Figure 1). The red molecule corresponds to NPC-up molecule, although the lobes corresponding to the “O” phenyl rings and clearly observed in Figure 1g were missing. The outer parts of the NPC-up molecules were not observed when they were close to a Pc-up molecule.

A schematic model of the ordered film is shown in Figure 4b in which NPC-up and Pc-up molecules alternate. The nearest distance between the molecules was ~ 1.7 nm, which is smaller than that observed in the 1D chain.

We optimized the model of the 2D assembly of NPC-up and Pc-up molecules by using DFT calculations, the results of which are shown in Figure 4c. The azimuthal angles between NPC and Pc ligands (indicated by the red and gray lines) of both NPC-up and Pc-up molecules (37°) are 8° smaller than that of the isolated adsorbate. A simulated STM image is shown in Figure 4d. The eight outer lobes of the four “l” phenyl rings dominate the image, and the lobes from “O” and “l” of the NPC-up molecules are weaker. The simulated STM image reproduces the features of the experimental one.

The Kondo feature observed over the film is different from those over the isolated molecules and 1D chains. Plots of the dI/dV data obtained at the lobes of NPC-up and Pc-up molecules of the film are shown in Figure 4e. Neither of the two plots shows a Kondo feature. We believe that this is due to the loss of the $1/2$ spin from the molecules, which was supported by using spin-resolved DFT calculations. Figure 4f shows calculated plots of the PDOSs for up- and down-spin components, which are shown as red and black curves, respectively. Although in the plots in Figure 2c, an unpaired spin was observed in a π orbital, in Figure 4f, no spin polarization was observed, explaining the disappearance of the Kondo feature.

We have previously discussed a mechanism of the disappearance of the $1/2$ spin of TbPc_2 molecule when the relative azimuthal angle of two Pc molecules (θ) is rotated from 45° to 30° .¹⁷ As θ decreases from 45° , the SOMO and HOMO become closer in energy. We examine whether a similar mechanism works for Pc–NPC ligands.

This can be estimated by a DFT calculation by observing energy levels of SOMO and HOMO states as a function of the relative azimuthal angle of NPC and Pc ligands. The result calculated for an isolated TbNPCpC molecule in vacuum is shown in Figure 4g. The decrease of the SOMO–HOMO gap with θ can be seen, which is similar to the case of the TbPc_2 molecule.¹⁷ However, the energy variation for the θ change from 45° to 37° is much smaller than that calculated for the TbPc_2 molecule when θ change from 45° to 30° . Instead of the

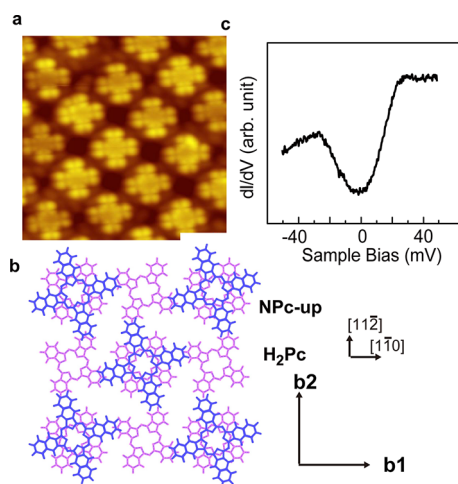


Figure 5. (a) STM image of a film composed of a mixture of TbNPCpC and H_2Pc molecules. White bar = 2 nm. (b) Model of molecular assembly. Violet and blue correspond to NPC and Pc, respectively. See text for lattice vector **b1** and **b2**. (c) dI/dV spectra obtained at the ligand of the NPC-up molecule.

approach of the SOMO and HOMO levels, we consider enhanced overlapping of molecules due to the smaller molecule–molecule distance in the 2D lattice which caused the disappearance of the spin as was demonstrated in the spin-resolved DOS plot in Figure 4f.

Here we show that more variety of molecular assemblies can be formed by combining a family of phthalocyanine molecules. In Figure 5a, we show an STM image of a film when a mixture of TbNPCpC and H_2Pc molecules was sublimated onto a Au(111) substrate. A pseudosquare ordering of NPC-up molecules can be seen, in which the NPC–NPC distance is ~ 2.0 nm. We constructed a model, which can reproduce the size of the lattice of NPC-up molecules and the rotational angle of the symmetry of NPC ligand, based on the pseudosquare lattice commonly observed for FePc ,³⁶ CoPc ,³⁷ and TbPc_2 molecules¹⁷ on the Au(111) surface. The lattice of the TbPc_2 film can be expressed with the vectors **b1** and **b2** shown in Figure 5b, in which **b1** is parallel to $[\bar{1}10]$ with a length of $5a$ (a is the nearest neighbor distance of Au atoms, $a \sim 0.288$ nm) and **b2** is parallel to $[11\bar{2}]$ with a length of $3\sqrt{3}a$.

In the film of the mixture of TbNPCpC and H_2Pc molecules, the TbNPCpC molecules form a checkerboard pattern occupying alternative sites, in which the angle of the Pc ligand is equivalent to that of H_2Pc molecules. The STM images only the TbNPCpC molecule.

The dI/dV spectra obtained over an NPC-up molecule are shown in Figure 5c, which showed a dip at the Fermi level. The shape of the dip was close to the one observed for the 1D chain of NPC-up molecules. The distance of neighboring NPC-up molecules were ~ 2.2 and ~ 2.0 nm for the 1D chain and $\text{TbNPCpC}/\text{H}_2\text{Pc}$ mixture, which might have made a similar overlapping between NPC ligands.

CONCLUSIONS

We studied the heteroleptic double-decker complex TbNPCPc (NPC = naphthalocyaninato and Pc = phthalocyaninato), in which an unpaired π electron causes Kondo resonance upon adsorption on a Au(111) surface. Two types of adsorption geometries appear depending on which side contacts the substrate surface, which are called NPC-up and Pc-up molecules. Their mixture makes intriguing molecular assemblies by segregation, including straight chains only of NPC-up molecules, and a film in which NPC-up and Pc-up molecules alternate.

In dI/dV spectra, a Kondo resonance was detected when the STM tip was over ligands of isolated NPC-up and Pc-up molecules, which showed different Kondo temperatures. The Kondo peak was converted into a

dip at the Fermi level in the 1D chain and disappeared in the 2D film. Sublimation of double-decker complexes with different ligands is a straightforward method to realize a segregation on surfaces. The simplicity of this method will make it possible to form more complex molecular assemblies by controlling the interactions of the upper and lower ligands. Moreover, domains with different spin properties, such as Kondo resonances, formed using this method. In other words, the adsorption configuration controls not only a molecule ordered structure but also Kondo temperature and the peak dip structure of Kondo resonance in dI/dV spectra. This implies that spin-mediated control of the electronic conductance of the molecule can be made by combining molecular design and adsorption tailoring.

METHODS

A 2,3-naphthalocyaninato phthalocyaninato Tb(III) double-decker complex (TbNPCPc) was synthesized following a previously reported method, which is described in detail in the Supporting Information.

We transferred the molecule to a substrate by using a sublimation method in an ultrahigh vacuum (UHV). Substrate cleaning, molecule deposition, and low-temperature STM observations were carried out in UHV chambers, whose details are described elsewhere.^{38,39} The sample temperature was ~ 4.7 K for the scanning tunneling microscopy (STM)/STS experiments described in this report. STS spectra were obtained using a lock-in amplifier with a modulation voltage of 1 mV superimposed onto the tunneling bias voltage.

First-principle calculations were performed by using VASP code, employing a plane wave basis set and PAW potentials in order to describe the behavior of the valence electrons.^{40,41} A generalized gradient Perdew–Burke–Ernzerhof (PBE) exchange–correlation potential⁴² was used. The structures were relaxed until the forces were smaller than 0.05 eV/Å. Due to the absence of dispersion forces in the local and semilocal exchange–correlation approximations, the molecule–surface distance of a weak bonding case such as van der Waals interaction is still controversial, which is followed by an ambiguity of the charge transfer from the substrate to the molecule. Nevertheless, the calculation results for the adsorbed molecule with van der Waals interactions give an accuracy good enough to understand the spin behavior if compared with the result calculated for the molecules placed in the vacuum. The gold surface was modeled as a five atom thick slab. The Tersoff and Hamman theory⁴³ was used to compute the STM images using a previously reported method.⁴⁴

Conflict of Interest: The authors declare no competing financial interest.

Acknowledgment. This work was financially supported by a Grant-in-Aid for Scientific Research (S) (Grant No. 20225003) for M.Y., a Grant-in-Aid for Scientific Research (A) (Grant No. 22241026) for T.K., and a Grant-in-Aid for Young Scientists (B) (Grant No. 24750119) for K.K. from the Ministry of Education, Culture, Sports, Science, and Technology, Japan.

Supporting Information Available: Spin-resolved PDOS calculation for 1D chain of NPC molecule and synthesis of unsymmetrical double-decker 2,3-naphthalocyaninato phthalocyaninato Ln(III) complexes (Ln = Tb³⁺ and Y³⁺) are presented. This material is available free of charge via the Internet at <http://pubs.acs.org>.

REFERENCES AND NOTES

- Bogani, L.; Wernsdorfer, W. Molecular Spintronics Using Single-Molecule Magnets. *Nat. Mater.* **2008**, *7*, 179–186.
- Barth, J. V.; Weckesser, J.; Lin, N.; Dmitriev, A.; Kern, K. Supramolecular Architectures and Nanostructures at Metal Surfaces. *Appl. Phys. A* **2003**, *76*, 645–652.
- Spillmann, H.; Dmitriev, A.; Lin, N.; Messina, P.; Barth, J. V.; Kern, K. Hierarchical Assembly of Two-Dimensional Homochiral Nanocavity Arrays. *J. Am. Chem. Soc.* **2003**, *125*, 10725–10728.
- Kondo, J. Effect of Ordinary Scattering on Exchange Scattering from Magnetic Impurity in Metals. *Phys. Rev.* **1968**, *169*, 437–440.
- Madhavan, V.; Chen, W.; Jamneala, T.; Crommie, M. F.; Wingreen, N. S. Tunneling into a Single Magnetic Atom: Spectroscopic Evidence of the Kondo Resonance. *Science* **1998**, *280*, 567–569.
- Li, J. T.; Schneider, W. D.; Berndt, R.; Delley, B. Kondo Scattering Observed at a Single Magnetic Impurity. *Phys. Rev. Lett.* **1998**, *80*, 2893–2896.
- Manoharan, H. C.; Lutz, C. P.; Eigler, D. M. Quantum Mirages Formed by Coherent Projection of Electronic Structure. *Nature* **2000**, *403*, 512–515.
- Knorr, N.; Schneider, M. A.; Diekhoner, L.; Wahl, P.; Kern, K. Kondo Effect of Single Co Adatoms on Cu Surfaces. *Phys. Rev. Lett.* **2002**, *88*, 096804.
- Wahl, P.; Diekhoner, L.; Wittich, G.; Vitali, L.; Schneider, M. A.; Kern, K. Kondo Effect of Molecular Complexes at Surfaces: Ligand Control of the Local Spin Coupling. *Phys. Rev. Lett.* **2005**, *95*, 166601.
- Neel, N.; Kroger, J.; Limot, L.; Palotas, K.; Hofer, W. A.; Berndt, R. Conductance and Kondo Effect in a Controlled Single-Atom Contact. *Phys. Rev. Lett.* **2007**, *98*, 016801.
- Zhao, A. D.; Li, Q. X.; Chen, L.; Xiang, H. J.; Wang, W. H.; Pan, S.; Wang, B.; Xiao, X. D.; Yang, J. L.; Hou, J. G.; *et al.* Controlling the Kondo Effect of an Adsorbed Magnetic Ion through Its Chemical Bonding. *Science* **2005**, *309*, 1542–1544.
- Iancu, V.; Deshpande, A.; Hla, S. W. Manipulation of the Kondo Effect via Two-Dimensional Molecular Assembly. *Phys. Rev. Lett.* **2006**, *97*, 266603.
- Chen, L.; Hu, Z. P.; Zhao, A. D.; Wang, B.; Luo, Y.; Yang, J. L.; Hou, J. G. Mechanism for Negative Differential Resistance in Molecular Electronic Devices: Local Orbital Symmetry Matching. *Phys. Rev. Lett.* **2007**, *99*, 146803.
- Jarillo-Herrero, P.; Kong, J.; van der Zant, H. S. J.; Dekker, C.; Kouwenhoven, L. P.; De Franceschi, S. Orbital Kondo Effect in Carbon Nanotubes. *Nature* **2005**, *434*, 484–488.

15. Fernandez-Torrente, I.; Franke, K. J.; Pascual, J. I. Vibrational Kondo Effect in Pure Organic Charge-Transfer Assemblies. *Phys. Rev. Lett.* **2008**, *101*, 217203.
16. Jeong, H.; Chang, A. M.; Melloch, M. R. The Kondo Effect in an Artificial Quantum Dot Molecule. *Science* **2001**, *293*, 2221–2223.
17. Komeda, T.; Isshiki, H.; Liu, J.; Zhang, Y.-F.; Lorente, N. S.; Katoh, K.; Breedlove, B. K.; Yamashita, M. Observation and Electric Current Control of a Local Spin in a Single-Molecule Magnet. *Nat. Commun.* **2011**, *2*, 217.
18. Nagaoka, K.; Jamneala, T.; Grobis, M.; Crommie, M. F. Temperature Dependence of a Single Kondo Impurity. *Phys. Rev. Lett.* **2002**, *88*, 077205.
19. Schlottmann, P. Some Exact Results for Dilute Mixed-Valent and Heavy-Fermion Systems. *Phys. Rep.* **1989**, *181*, 1–119.
20. Hewson, A. C. *The Kondo Problem to Heavy Fermions*; Cambridge University Press: London, 1993.
21. Auerhammer, J. M.; Knupfer, M.; Peisert, H.; Fink, J. The Copper Phthalocyanine/Au(100) Interface Studied Using High Resolution Electron Energy-Loss Spectroscopy. *Surf. Sci.* **2002**, *506*, 333–338.
22. Persson, B. N. J.; Baratoff, A. Inelastic Electron Tunneling from a Metal Tip: The Contribution from Resonant Processes. *Phys. Rev. Lett.* **1987**, *59*, 339.
23. Lorente, N.; Persson, B. N. J.; Lauhon, L. J.; Ho, W. Symmetry Selection Rules for Vibrationally Inelastic Tunneling. *Phys. Rev. Lett.* **2001**, *86*, 2593–2596.
24. Ishikawa, N.; Sugita, M.; Okubo, T.; Tanaka, N.; Lino, T.; Kaizu, Y. Determination of Ligand-Field Parameters and F-Electronic Structures of Double-Decker Bis(phthalocyaninato)-lanthanide Complexes. *Inorg. Chem.* **2003**, *42*, 2440–2446.
25. Komeda, T.; Isshiki, H.; Liu, J. Metal-Free Phthalocyanine (H₂Pc) Molecule Adsorbed on the Au(111) Surface: Formation of a Wide Domain along a Single Lattice Direction. *Sci. Technol. Adv. Mater.* **2010**, *11*, 054602.
26. Tsukahara, N.; Noto, K. I.; Ohara, M.; Shiraki, S.; Takagi, N.; Takata, Y.; Miyawaki, J.; Taguchi, M.; Chainani, A.; Shin, S.; *et al.* Adsorption-Induced Switching of Magnetic Anisotropy in a Single Iron(II) Phthalocyanine Molecule on an Oxidized Cu(110) Surface. *Phys. Rev. Lett.* **2009**, *102*, 167203.
27. Fano, U. Effects of Configuration Interaction on Intensities and Phase Shifts. *Phys. Rev.* **1961**, *124*, 1866–1878.
28. Ujsaghy, O.; Kroha, J.; Szunyogh, L.; Zawadowski, A. Theory of the Fano Resonance in the STM Tunneling Density of States Due to a Single Kondo Impurity. *Phys. Rev. Lett.* **2000**, *85*, 2557–2560.
29. Piihal, M.; Gadzuk, J. W. Nonequilibrium Theory of Scanning Tunneling Spectroscopy via Adsorbate Resonances: Nonmagnetic and Kondo Impurities. *Phys. Rev. B* **2001**, *63*, 085404.
30. DiLullo, A.; Chang, S.-H.; Baadji, N.; Clark, K.; Klöckner, J.-P.; Prosen, M.-H.; Sanvito, S.; Wiesendanger, R.; Hoffmann, G.; Hla, S.-W. Molecular Kondo Chain. *Nano Lett.* **2012**, *12*, 3174–3179.
31. Iancu, V.; Deshpande, A.; Hla, S. W. Manipulating Kondo Temperature via Single Molecule Switching. *Nano Lett.* **2006**, *6*, 820–823.
32. Aguiar-Hualde, J. M.; Chiappe, G.; Louis, E.; Anda, E. V.; Simonin, J. Kondo Resonance in the Conductance of Copc/Au(111) and Tbrpp-Co/Cu(111). *Phys. Rev. B* **2009**, *79*, 155415.
33. Aguiar-Hualde, J. M.; Chiappe, G.; Louis, E.; Anda, E. V.; Simonin, J. Modeling the Effects of Molecule Distortion on the Kondo Resonance in the Conductance of CoPc/Au(111) and Tbrpp-Co/Cu(111). *Phys. Status Solidi A* **2009**, *206*, 2217–2227.
34. Aguiar-Hualde, J. M.; Chiappe, G.; Louis, E.; Anda, E. V. Kondo Effect in Transport through Molecules Adsorbed on Metal Surfaces: From Fano Dips to Kondo Peaks. *Phys. Rev. B* **2007**, *76*, 155427.
35. Gopakumar, T. G.; Brumme, T.; Kroger, J.; Toher, C.; Cuniberti, G.; Berndt, R. Coverage-Driven Electronic Decoupling of Fe-Phthalocyanine from a Ag(111) Substrate. *J. Phys. Chem. C* **2011**, *115*, 12173–12179.
36. Gao, L.; Ji, W.; Hu, Y. B.; Cheng, Z. H.; Deng, Z. T.; Liu, Q.; Jiang, N.; Lin, X.; Guo, W.; Du, S. X.; *et al.* Site-Specific Kondo Effect at Ambient Temperatures in Iron-Based Molecules. *Phys. Rev. Lett.* **2007**, *99*, 106402.
37. Takada, M.; Tada, H. Low Temperature Scanning Tunneling Microscopy of Phthalocyanine Multilayers on Au(111) Surfaces. *Chem. Phys. Lett.* **2004**, *392*, 265–269.
38. Zhang, Y. F.; Isshiki, H.; Katoh, K.; Yoshida, Y.; Yamashita, M.; Miyasaka, H.; Breedlove, B. K.; Kajiwara, T.; Takaishi, S.; Komeda, T. A Low-Temperature Scanning Tunneling Microscope Investigation of a Nonplanar Dysprosium-Phthalocyanine Adsorption on Au(111). *J. Phys. Chem. C* **2009**, *113*, 14407–14410.
39. Zhang, Y. F.; Isshiki, H.; Katoh, K.; Yoshida, Y.; Yamashita, M.; Miyasaka, H.; Breedlove, B. K.; Kajiwara, T.; Takaishi, S.; Komeda, T. Low-Temperature Scanning Tunneling Microscopy Investigation of Bis(phthalocyaninato)yttrium Growth on Au(111): From Individual Molecules to Two-Dimensional Domains. *J. Phys. Chem. C* **2009**, *113*, 9826–9830.
40. Kresse, G.; Furthmüller, J. Efficient Iterative Schemes for *Ab Initio* Total-Energy Calculations Using a Plane-Wave Basis Set. *Phys. Rev. B* **1996**, *54*, 11169–11186.
41. Kresse, G.; Joubert, D. From Ultrasoft Pseudopotentials to the Projector Augmented-Wave Method. *Phys. Rev. B* **1999**, *59*, 1758–1775.
42. Perdew, J. P.; Burke, K.; Ernzerhof, M. Generalized Gradient Approximation Made Simple. *Phys. Rev. Lett.* **1996**, *77*, 3865–3868.
43. Tersoff, J.; Hamann, D. R. Theory and Application for the Scanning Tunneling Microscope. *Phys. Rev. Lett.* **1983**, *50*, 1998–2001.
44. Bocquet, M.-L.; Lesnard, H.; Monturet, S.; Lorente, N. Theory of Elastic and Inelastic Electron Tunneling. In *Computational Methods in Catalysis and Materials Science*, van Santen, R. A., Sautet, P., Eds.; Wiley-VCH: Weinheim, Germany, 2009; ISBN 978-3-527-32032-5; p 201.